

REPORT DOCUMENTATION PAGE

AFRL-SR-BL-TR-00

The public reporting burden for this collection of information is estimated to average 1 hour per response, including gathering and maintaining the data needed, and completing and reviewing the collection of information. Send comments regarding this burden estimate or any other aspect of this collection of information, including suggestions for reducing the burden, to Department of Defense, Washington Headquarters, 1215 Jefferson Davis Highway, Suite 1204, Arlington, VA 22202-4302. Respondents should be subject to any penalty for failing to comply with a collection of information if it does not display a currently valid OMB control number.

purpose,
section
reports
shall be

0009

1. REPORT DATE (DD-MM-YYYY) 7-12-1999		2. REPORT TYPE Final Technical		3. DATES COVERED (From - To) 01/8/1996 - 31/7/1999	
4. TITLE AND SUBTITLE Atomistic and AB Initio Calculations of Ternary II-IV-V2 Semiconductors				5a. CONTRACT NUMBER	
				5b. GRANT NUMBER F49620-96-0319	
				5c. PROGRAM ELEMENT NUMBER	
6. AUTHOR(S) Ravi Pandey				5d. PROJECT NUMBER 2305/EX	
				5e. TASK NUMBER 2305/EX	
				5f. WORK UNIT NUMBER	
7. PERFORMING ORGANIZATION NAME(S) AND ADDRESS(ES) Michigan Technological University 1400 Townsend Drive Houghton, MI 49931				8. PERFORMING ORGANIZATION REPORT NUMBER	
9. SPONSORING/MONITORING AGENCY NAME(S) AND ADDRESS(ES) AFOSR/NE 20000114 045				10. SPONSOR/MONITOR'S ACRONYM(S) AFOSR/NE - Johnstone	
				11. SPONSOR/MONITOR'S REPORT NUMBER(S)	
12. DISTRIBUTION/AVAILABILITY STATEMENT Approved for Public release; distribution unlimited					
13. SUPPLEMENTARY NOTES					
14. ABSTRACT Atomistic and <i>ab initio</i> methods are used to study structural and electronic properties of perfect and defective chalcopyrites, specifically, ZnGeP_2 and CdGeAs_2 . These materials are important due to their suitability for nonlinear optical applications in the infrared region and have a wide transparency region. A new set of interatomic potential parameters consisting of two- and three-body terms is developed reproducing crystal lattice constants, elastic and dielectric constants very well. The calculated formation energies for native defects suggest that the intrinsic disorder is dominated by antisites in the cation sublattice followed by the Schottky and Frenkel defects. Although both compounds belong to the same chalcopyrite family, the nature of dominant acceptors is predicted to be different. Defect calculations corroborating the experimental studies find that the zinc vacancy, not the zinc antisite (Zn_{Ge}), is associated with the dominant acceptor center in ZnGeP_2 . This is not the case in CdGeAs_2 where a cadmium antisite (Cd_{Ge}) is predicted to be associated with the dominant acceptor in the lattice. This difference may well be due to defect-induced lattice distortion which plays a key role in stabilizing the hole states in the lattice.					
15. SUBJECT TERMS Chalcopyrites, Defects, Atomistic and AB Initio Calculations					
16. SECURITY CLASSIFICATION OF:			17. LIMITATION OF ABSTRACT UU	18. NUMBER OF PAGES 60	19a. NAME OF RESPONSIBLE PERSON R. PANDEY
a. REPORT U	b. ABSTRACT U	c. THIS PAGE U			19b. TELEPHONE NUMBER (Include area code) (906) 487-2831

Standard Form 298 (Rev. 8/98)
Prescribed by ANSI Std. Z39.18

Cover Page for Final Technical Report

Report Submitted to: Maj. D. Johnstone, AFOSR/NE
110 Duncan Avenue, Suite B 115
Bolling AFB, DC 20332-0001

Date Submitted: Dec. 7, 1999

Grant No. : F49620-96-1-0319


Legal Institution Name: Michigan Technological University
1400 Townsend Drive
Houghton, MI 49931

Principal Investigator: Ravi Pandey
Physics Department
(906) 487 2831; E mail : pandey@mtu.edu

Business Office: Michigan Technological University
1400 Townsend Drive
Houghton, MI 49931-1295

Principal Investigator:
Title
Phone Number

Ravi Pandey
Professor
(906) 487 2831



12/7/99

Date

Executive Summary

This documentation is the final technical report for work performed under AFOSR grant F49620-96-1-0319. The title of this project was "Atomistic and Ab Initio Calculations of Ternary II-IV-V₂ semiconductors" and the Principal Investigator was Ravi Pandey, Physics Department, Michigan Technological University, Houghton, MI 49931. It was 36-months research program to use atomistic and first-principles methods to study chalcopyrites and related semiconducting materials. During the grant's active period, the following reports have been published :

- (i) M. Ohmer and R. Pandey (Guest Editors), MRS Bulletin July 1998
"Emergence of chalcopyrites as nonlinear optical materials."
- (ii) P. Zapol, R. Pandey, M. Seel, J. M. Recio and M. Ohmer and J. M. Recio 1999,
J. Phys : Condensed Matter 11, 1.
"Density functional study of the structure, thermodynamics and electronic properties of CdGeAs₂."
- (iii) R. Pandey, M. Ohmer and J. Gale, 1998, J. Phys : Condensed Matter 10, 5525.
"A theoretical study of native acceptors in CdGeAs₂."
- (iv) R. Pandey, M. Ohmer, A. Costales and J. M. Recio, 1998, MRS Symposium Proceedings Volume 484, p.525.
"Atomistic calculations of dopant binding energies in ZnGeP₂."
- (v) R. Pandey, M. Ohmer, A. Costales and J. M. Recio, 1999, MRS Symposium Proceedings, Submitted.
"Modeling of dopant properties in CdGeAs₂."
- (vi) P. Zapol, R. Pandey and J. Gale, 1997, J. Phys. Condensed Matter 9, 9517.
"An interatomic potential study of the properties of GaN."
- (vii) R. Pandey, P. Zapol and M. Causa, 1997, Phys. Rev. B 55, R16009.
"A theoretical study of nonpolar surfaces of AlN."
- (viii) R. Pandey, M. Rerat and M. Causa, 1999, Appl. Phys Letts. 75, In Press.
"First-principles study of stability, band structure, and optical properties of the ordered Ge_{0.50}Sn_{0.50} alloy."

Interactions/Transitions with U. S. Air Force Research Laboratory :

1. Co-edited an issue of MRS Bulletin (July 1998) with Mel Ohmer (Wright Lab) on NLO Chalcopyrites.
2. Organized a session on NLO materials in the MRS Fall meeting, 1997.
3. Sabbatical leave, Wright Laboratory, Dayton, 1997.
4. Summer visit to Wright Laboratory, Dayton, 1998.

5. Summer visit to Wright Laboratory, Dayton, 1999.
6. Co-organizer of a US-UK-Russia workshop on NLO semiconductors with Mel Ohmer and Tony Vere, Malvern, UK. Sept. 1999.

Honors/Awards

National Research Council Senior Fellowship, 1997.

Student Supported :

Peter Zapol, Ph. D., 1996-98.

Currently, Peter is a post-doctoral research associate at Argonne National Laboratory, Chicago.

Accomplishments/New Findings :

(1) Atomistic defect calculations in ZnGeP_2 have identified the dominant native acceptor to be the zinc acceptor vacancy which is responsible for the presence of absorption band near the pump wavelength limits. Although cation lattice disorder is predicted to be the dominant native defect, the dominant defects controlling the properties of interest would seem to be the zinc acceptor vacancy (binding energy of 0.57 eV) which is partially compensated by a phosphorus donor vacancy (binding energy of 0.68 eV). For the EPR-active acceptor center, the calculated binding energies and lattice distortion corroborates the ENDOR spectrum associating the zinc vacancy with the acceptor center.

(2) In CdGeAs_2 , the acceptor center identified by Hall-effect measurements and EPR is found to be related to the delocalized hole shared by the four As neighbors bound to Cd_{Ge} . For this center, calculations yield a binding energy of 0.13 eV in an agreement with the experimental value of 0.15 eV obtained by the Hall-effect measurements.

Although ZnGeP_2 and CdGeAs_2 belong to the same chalcopyrite family, the nature of dominant acceptors in these materials is predicted to be different. Defect calculations corroborating the Hall effect (Ohmer) and magnetic resonance (Halliburton) studies find that the zinc vacancy, not the zinc antisite (Zn_{Ge}), is associated with the dominant acceptor center in ZnGeP_2 . This is not the case in CdGeAs_2 where a cadmium antisite (Cd_{Ge}) is predicted to be associated with the dominant acceptor in the lattice. We believe that this difference may well be due to defect-induced lattice distortion which plays a key role in stabilizing the hole states in the lattice.

(3) ZnGeP_2 is the NLO material for mid IR lasers allowing high-power tunability in the spectral region of 2-5 μm . An absorption band around 1-2 μm is, however, found to affect the usefulness of ZnGeP_2 . Experimental efforts involving selective doping of ZnGeP_2 are underway at Lockheed to reduce the concentration of the acceptor-complex giving rise to an absorption band around 1-2 μm in the lattice. To provide a guidance to experimental efforts, we have performed atomistic calculations on ZnGeP_2 involving cation dopants, namely Cu, Ag, B, Al, Ga and In. Calculations predict small binding energies for Cu and Ag substituting Zn in the lattice which are in agreement with the available experimental data. The group III dopants (i.e. B, Al, Ga and In) at the Ge site are predicted to have large binding energies for a hole except B which shows a distinct behavior. This is due to large mismatch in atomic sizes of B and Ge. At

the Zn site, the calculated binding energies of the group III dopants place donor levels in the middle of the band gap.

(4) Group-IV semiconductor alloys have immense potential for applications in the next generation of Si-based electronic and photonic devices. The MBE group at Michigan Tech funded by DARPA has recently reported (Phys Rev Lett 80, 1022 (1998)) the morphological evolution of an epitaxially strained Ge-Sn alloy thin films. Since a knowledge of structural, electronic and optical properties of GeSn alloys is critical in promoting alloy thin films for device applications, we have performed a first-principles study on the ordered $\text{Ge}_{0.50}\text{Sn}_{0.50}$ alloy. The results show a relative stability of the ordered alloy for which the lattice constant and the bulk modulus are predicted to be 6.20 Å and 53 GPa, respectively. Analysis of band structure and density of states shows the alloy to be *direct-gap* semiconductor with the value of 4.44 for the index of refraction at 6889 nm.

CONTENTS

Cover Page(i)
Executive Summary(ii)
First Principles Study of CdGeAs ₂1
Atomistic Modeling of Native Defects in CdGeAs ₂24
Atomistic calculations of dopant binding energies in ZnGeP ₂39
First-principles study of the ordered Ge _{0.50} Sn _{0.50} alloy47

First Principles Study of CdGeAs₂.

1 Introduction

Since the first CdGeAs₂ crystals were grown⁶ in the early 70s, their bulk properties have attracted much attention. The photoluminescence studies have revealed the detailed information about the nature of its band gap.⁷ The electrical and Hall effect measurements have determined the nature of charge carriers in this material.^{9,8} The presence of at least two native acceptors has been observed in experiments utilizing radiation damage,¹⁰ magnetic resonance¹¹ and thermal admittance spectroscopy¹² techniques. Bulk modulus and Debye temperature were also obtained from measurements of the ultrasonic wave velocities.¹³ On the theoretical front, empirical pseudopotential calculations have focused only on its band structure.^{15,16} Although calculations based on first-principles methods have been performed on several members of the chalcopyrite group,^{17,18} we are not aware of any such calculations on CdGeAs₂.

In this section, we report the results of calculations based on the density functional theory on CdGeAs₂ with the aim (i) to provide a detailed information about its electronic structure, (ii) to determine its thermodynamic properties within a Debye-like model, and (iii) to combine knowledge of electronic structure and thermodynamics to determine pressure dependence of its band structure. In the following section, computational details will be

given. Results will be discussed in Sec. IV.

2 Computational Details

Electronic structure calculations of CdGeAs_2 are based on the density functional theory embedded in the CRYSTAL95 program¹⁹ which has been successful in describing bulk and surface properties of covalent materials such as Si and GaN.^{20,21} We perform calculations in the framework of the local density approximation^{23,22} (LDA) to the density-functional theory (DFT). In some cases, gradient-corrected functionals (GGA), Becke²⁴ for exchange and Perdew and Wang^{25,26} for correlation, are employed to see the effect of these corrections on the calculated structural properties.

A linear combination of Gaussian orbitals are used to generate a localized atomic basis from which Bloch functions are constructed by a further linear combination with plane-wave phase factors. To reduce the computational cost in the present work, we represent the core electrons by Steven's effective core potentials (ECPs)^{27,28} and describe the respective valence electrons by the corresponding Gaussian basis set. The core electrons for Cd, Ge and As are $1s^2$, $2s^2$, $2p^6$, $3s^2$, $3p^6$ and $3d^{10}$. It has been shown that the ECPs (such as for Zn and Ge used in this work) derived from the Hartree-Fock calculations provide satisfactory description of the ground state properties in the DFT calculations.²⁹ The Gaussian basis set consists of four s, four p and three d-type shells for Cd (i.e. a 4121/4121/311 set), two s, two p and

a d-type shell for Ge (i.e. a 41/41/1 set), and two s, two p and a d-type shell for As (i.e. a 41/41/1 set). It is to be noted here that the outermost 4d electrons of Cd are considered explicitly here as valence electrons and are not included in the ECPs. Furthermore, the outer exponents in each of the basis set are reoptimized to yield the minimal total energy at the experimental geometry of CdGeAs₂.

The initial configuration for the geometry optimization is taken from the X-ray diffraction data. At ambient conditions, CdGeAs₂ crystallizes in the chalcopyrite phase^{30,31} with a space group of I-42D. It can be constructed⁷ by first considering a superlattice of the (cubic) zincblende phase with $c/a=2$, replacing each half of cations by Cd and Ge ions respectively and finally introducing a small distortion along z-axis leading to $c/a = 1.889$. Furthermore, the As atoms are placed in the lattice in the special positions given by the internal parameter, u , which is related to the tetragonal distortion (i.e. $2-(c/a)$) in the lattice. Geometry optimization calculations in the LDA approximation therefore involve the following steps: (i) for several fixed values of the crystallographic unit cell volume, ranging approximately from 0.8 to 1.08 times the experimental one, the lattice constant a and the internal parameter u is optimized with accuracies better than 10^{-3} Å and 10^{-4} , respectively; (ii) the calculated potential energy surface (i.e. total energy *vs* volume) is then used to obtain the optimized value of the unit cell volume; and (iii) the optimization of a and u is again performed at this

volume to get the values of equilibrium structural parameters. In the GGA calculations, geometry optimization is achieved by a less -exhaustive approach where series of one dimensional searches are performed varying each structural parameters (i.e. a , c and u) one by one on each step, repeating the steps until convergence of 0.01 Å in the parameter value is achieved. In all of these calculations, the tolerance on the total energy convergence in the iterative solution of the Kohn-Sham equations is set to 10^{-6} Hartree and a grid of 59 k -points was used in the irredicible Brillouin Zone for integration in the reciprocal space.³²

3 Structural and Electronic Properties

The calculated equilibrium values of the structural parameters, namely a , c/a and u for CdGeAs₂ are 5.914 Å, 1.915 and 0.265 in the LDA approximation and 5.94 Å, 1.89 and 0.265 in the GGA approximation respectively. On the other hand, the experimental values of the lattice parameters,³¹ a and c , are 5.9432 Å and 11.2163 Å respectively at 298 K leading to the c/a ratio of 1.887. Comparison between the GGA and experimental values of the lattice constants shows an excellent agreement. The calculated LDA unit cell volume is also well within 1% of the experimental value. However, the LDA calculations yield slight underestimation of a and overestimation the c/a ratio as expected. Both LDA and GGA values of the internal parameter u are lower than the experimental value of 0.2785. This is in accordance with the

results of the LDA calculations on ZnGeP_2 , CdSnP_2 and CdSnAs_2 where the calculated u is consistently lower than the corresponding experimental value.¹⁸ It is to be noted here that the X-ray diffraction studies obtain the value of the internal parameter, u , only in an indirect way.⁷

The calculated interatomic distance between Cd-As and Ge-As is 2.579 and 2.474 Å at the LDA level and 2.581 and 2.477 Å at the GGA level, respectively. It has been suggested that the tetrahedral angle in the chalcopyrite lattice is generally conserved by the group-IV atom (i.e. Ge). This results in a larger separation between the group II and the group V atoms relative to the group IV and the group V atoms in the lattice. This is what has been predicted by our calculations in CdGeAs_2 . Assuming the conservation of tetrahedral bond radii, Jaffe and Zunger³³ have reported the structural coordinates of chalcopyrites. In this scheme, the calculated Cd-As and Ge-As distance comes out to be 2.63 and 2.45 Å respectively. We note here that the LDA calculations¹⁸ in CdSnAs_2 yield the Cd-As distance to be 2.611 Å.

Fig. 1 displays the upper valence and lower conduction band structure of CdGeAs_2 calculated at the LDA equilibrium geometry. Total and partial density of states of the valence band are shown in Fig. 2. Accordingly, the upper valence band is mainly formed by the As p states with very small admixture of the Ge p states and the Cd p states (Fig. 2). This band has a width of about 5.5 eV. In the absence of the spin-orbit interaction

terms in the present work, the top of the valence band consists of two levels having symmetry Γ_{5v} and Γ_{4v} ; the former being double degenerate. Both levels originate from the same triple degenerate Γ_{15} level of the sphalerite structure. The difference between the Γ_{5v} and Γ_{4v} levels is referred to as the crystal-field splitting (Δ_{cf}) which is calculated to be 0.33 eV. The corresponding experimental value is reported to be 0.21 eV.⁷

At about 9 eV below the top of the valence band (Fig. 2), a relatively narrow Cd 4*d* band overlaps with the band representing the bonding between the Ge and As in the lattice. Interestingly, the LDA calculations¹⁸ on CdSnP₂ reported the Cd 4*d* band to be at about -8.5 eV relative to the valence band maximum. However, we note here that the DFT calculations in the absence of self-interaction correction tend to underestimate the location of the *d* band with reference to the top of the valence band. Fig. 2 also shows a band at about -11 eV attributed mainly to the As *s* orbitals which appear to be hybridized with the Cd and Ge orbitals. Relative to the valence band maximum, we have collected the energies of the electronic states at Γ , *T* and *N* k-points⁷ that correspond to maxima and minima of the valence and conduction bands in Table 1.

In contrast to a very reasonable description of valence states, one-electron solutions of Kohn-Sham equations corresponding to the states in the conduction band are known to be much less reliable. The most evident and well-known discrepancy is a severe underestimation of the forbidden band

gap. For example, the calculated band gap in the present work for CdGeAs₂ is 0.16 eV as compared to the experimental value of 0.61 eV. This discrepancy may be corrected by employing a semiempirical correction³⁴ which simply shifts states in the conduction band using the following equation :

$$\Delta = \frac{9\text{eV}}{\epsilon_{\infty}} \quad (1)$$

where ϵ_{∞} is the high-frequency dielectric constant of the material. For CdGeAs₂, ϵ_{∞} is about 11.0^{1,2,14} leading to the value of the gap to 0.98 eV (Table 2).

The lowest gap between top of the valence band to bottom of the conduction band is found to be at Γ . Thus, the present DFT calculations predicts the gap to be direct ($\Gamma_{4v}-\Gamma_{1c}$) in agreement with experimental and empirical pseudopotential studies.¹⁵ The ordering of states in the conduction band (i.e. $\Gamma_{1c} < \Gamma_{3c} < \Gamma_{2c}$) is also correctly predicted. We note here that experimental assignments are only tentative because transitions to the last two states are only weakly allowed.

4 Thermodynamic properties

To determine thermodynamic properties of CdGeAs₂, we have used a quasi-harmonic Debye-like model in which the Debye temperature, Θ , depends only on the volume of the crystal. It is a non-empirical model that only needs the knowledge of the potential energy surface (i.e. a set of computed

($V, E_{latt}(V)$) points) to generate the equation of state (EOS) and a number of related quantities of a given material. It is relevant to notice that whereas the key parameters from the experimental point of view are pressure (p) and temperature (T), the appropriate variable to control the computation is volume (V). The computational strategy therefore includes optimization of the lattice constant a and the internal parameter u for several fixed values of the unit cell volume to obtain the energy surface. (see Sec. 2). Fig. 3 shows such energy surface for CdGeAs_2 calculated using the LDA approximation.

Assuming the isotropic conditions, Θ can be given by³⁵

$$\Theta = \frac{\hbar}{k_B} \left[6\pi^2 V^{\frac{1}{3}} r \right]^{\frac{1}{3}} \sqrt{\frac{B_S}{M}} f(\sigma) \quad (2)$$

where \hbar is the reduced Planck constant, k_B is the Boltzmann constant, M the molecular mass of the compound, r the number of atoms per molecular unit, B_S the adiabatic bulk modulus of the crystal, and σ the Poisson ratio which is taken to be 0.25, the value of the Cauchy solid.³⁵ The value of $f(\sigma = 0.25)$ then becomes 0.85995. Note that the explicit expression for $f(\sigma)$ in Eq. 2 is³⁵

$$f(\sigma) = \left\{ 3 \left[2 \left(\frac{2}{3} \frac{1+\sigma}{1-2\sigma} \right)^{\frac{3}{2}} + \left(\frac{1}{3} \frac{1+\sigma}{1-\sigma} \right)^{\frac{3}{2}} \right]^{-1} \right\}^{\frac{1}{3}} \quad (3)$$

In Eq. 2, B_S depends on V and T . In order to balance computational demand and accuracy, we further assume

$$B_S \simeq B_{\text{static}} = V \left(\frac{d^2 E_{latt}(V)}{dV^2} \right), \quad (4)$$

where B_{static} is the static bulk modulus.

Θ is now simply a function of V . It is also evident from Eqs. 2 and 4 that there is no explicit consideration of the structural parameters in the volume derivatives, since we restrict ourselves to hydrostatic conditions. This relevant feature of the model makes it fully independent of any particular crystal structure. Even if the crystal energy depends on many internal parameters and cell constants, a set of pairs (E_{latt}, V) is sufficient to employ the model. A more detailed description of the model is given in Ref. [34,35].

Our computed values of isothermal and adiabatic bulk moduli ($B_T(p = 0) = B_0$ and B_S) and their pressure and temperature derivatives are given in Table 3 along with the available experimental data. Fig. 4 shows the generated equation of state using the normalized $V(p)/V_0$ values, where V_0 is the corresponding equilibrium volume at zero pressure. It should be noted here that Hailing *et al*¹³ used the experimental bulk modulus and its first derivative obtained at pressures up to 0.1 GPa from ultrasonic measurements as parameters and did not fit the equation of state to the experimental curve. The higher experimental value of 69.7 GPa of B_0 relative to the calculated one of 57.0 GPa makes the simulated crystal to be more compressible, as illustrated in Fig. 4.

In the quasi-harmonic model used here, the Debye temperature, Θ_D , comes out to be 273K at the static equilibrium and 269K at room temperature. This variation is due to change of equilibrium volume with temper-

ature. On the other hand, the specific heat measurements³⁷ between 2K and 30K determine Θ_D to be 230K whereas the ultrasonic wave velocity experiment¹³ yields the value of 257K for Θ_D .

We note here that thermodynamic properties that are specially sensitive to computational details are those related to the volume dependence of Θ , since they involve third derivatives of the static lattice energy. The most important factor in computing this set of properties is the Grüneisen constant, γ . Our calculations yield γ to be 2.262 at 300K for CdGeAs₂. For the volume thermal expansion coefficient, α , the calculated value is $30.9 \times 10^{-6} \text{ K}^{-1}$ at 300K, and $33.8 \times 10^{-6} \text{ K}^{-1}$ at 400K as compared to the experimental value of $18 \times 10^{-6} \text{ K}^{-1}$.

The optical transitions in chalcopyrites are sensitive to applied hydrostatic pressure leading to dependence of the pressure coefficients on the nature of the band gap. For example, it has been found³⁸ that the pseudo-direct gap chalcopyrites,³⁹ such as ZnGeP₂, have a small positive or negative slope of the absorption edge, while CdGeAs₂ and other direct gap chalcopyrites have a large positive slope. Although the LDA calculations do not provide quantitative predictions of the band gap very well, they do provide reliable predictions of the change in gap under the hydrostatic conditions. For CdGeAs₂, we find that both valence and conduction levels at T , N and Γ k-points in the Brillouin zone show a linear variation with applied pressure up to 10 GPa. The calculated pressure coefficients⁴⁰ of these levels are given

in the Table 4 which yield the coefficient of the minimum-energy direct gap ($\Gamma_{4v}-\Gamma_{1c}$) to be 9.5×10^{-6} eV/bar. It is in very good agreement with the experimental value⁴¹ of 9.3×10^{-6} eV/bar. It is expected that knowledge of the pressure coefficients for different levels would assist experimentalists in identifying various optical transitions in CdGeAs₂.

In summary, we have calculated lattice constants, equation of state, Debye temperature, Grüneisen constant and electronic band structure of CdGeAs₂ in chalcopyrite structure which are in very good agreement with the available experimental data. The calculated results have also provided details of the valence and conduction bands predicting their variation with pressure.

References

- [1] R. L. Byer, H. Kildal, and R. S. Feigelson. *Appl. Phys. Lett.*, **19**, 237, 1971.
- [2] H. Kildal. *AFML-TR-72-277*. (Government technical report available from NTIS, AD739556), 1972.
- [3] G. D. Boyd, E. Buehler, F. Storz, and J. H. Wernick. *IEEE J. Quantum Electron.*, **8**, 419, 1972.
- [4] V. G. Dmitriev, G. G. Gurzadayan, and D. N. Nikogosyan. *Handbook of Nonlinear Optical Crystals*. Springer-Verlag, New York, 1997.

- [5] P. G. Schunemann and T. M. Pollak. *J. Cryst. Growth*, **174**, 215, 1997.
- [6] F. P. Kesamanly and Yu. V. Rud'. *Semiconductors*, **27**, 969, 1993.
- [7] J. L. Shay and J. H. Wernick. *Ternary Chalcopyrite Semiconductors: Growth, Electronic Properties and Applications*. Pergamon, Oxford, 1974.
- [8] D. W. Fischer, M. C. Ohmer and J. E. McCrae. *J. Appl. Phys.*, **81**, 3579, 1997.
- [9] V. Yu. Rud and Yu. V. Rud. *Jpn. J. Appl. Phys.*, **32**: Suppl. 32.3, 672, 1993.
- [10] V. N. Brudnyi, M. A. Krivov, A. I. Potapov, IO. K. Polushina, V. D. Prochukhan, Yu. V. Run. *Phys. Stat. Sol. (a)*, **49**, 761 1978.
- [11] L. E. Halliburton, G. J. Edwards, P. G. Schunemann and T. M. Pollak. *J. Appl. Phys.*, **77**, 435, 1994.
- [12] S. R. Smith, A. O. Ewaraye and M. C. Ohmer. *MRS Proceedings, Session F*, Fall 1997.
- [13] Tu Hailing, G. A. Saunders, W. A. Lambson, and R. S. Feigelson. *J. Phys. C: Solid State Phys.*, **15**, 1399, 1982.
- [14] R. Pandey, M. Ohmer, and J. D. Gale. *J. Phys. Condens. Matter*, **10**, 5525 (1998).

- [15] Yu. I. Polygalov and A. S. Poplavnoi. *Izv. Vuzov. Fizika*, **12**, 78, 1981.
- [16] R. Madelon, E. Paumier, and A. Hairie. *Physica Status Solidi (b)*, **165**, 435, 1991.
- [17] J. E. Jaffe and Alex Zunger. *Phys. Rev. B*, **30**, 741 (1984).
- [18] A. Continenza, S. Massidda, A. J. Freeman, T. M. de Pascale, F. Meloni, and M. Serra. *Phys. Rev. B*, **46**, 10070, 1992.
- [19] R. Dovesi, V. R. Saunders, C. Roetti, M. Causà, N. M. Harrison, R. Orlando, E. Aprà. *CRYSTAL95 User's Manual*, Universidad de Torino, 1996.
- [20] R. Pandey, M. Causà, N. M. Harrison, and M. Seel. *J. Phys. Condens. Matter*, **8**, 3993 (1996).
- [21] R. Pandey, P. Zapol and M. Causà. *Phys. Rev. B*, **55**, 1 (1997).
- [22] D. M. Ceperley and B. J. Alder. *Phys. Rev. Lett.*, **45**, 566, 1980.
- [23] J. P. Perdew and A. Zunger. *Phys. Rev. B.*, **23**, 5048, 1981.
- [24] A. D. Becke. *Phys. Rev. A*, **38**, 3098, 1988.
- [25] J. P. Perdew and Y. Wang. *Phys. Rev. B*, **33**, 8800, 1986.
- [26] J. P. Perdew and Y. Wang. *Phys. Rev. B*, **40**, 3399, 1989.
- [27] W. J. Stevens, H. Basch and M. Krauss. *J. Chem. Phys.*, **81**, 6026, 1985.

- [28] W. J. Stevens, M. Krauss, H. Basch and P. G. Jasien. *Canadian J. Chem.*, **37**, 2659, 1992.
- [29] M. Causà and A. Zupan *Int. J. Quantum Chem.*, **S28**, 633, 1994
- [30] A. S. Borshchevskii, N. A. Goryunova, F. P. Kesamanly and D. N. Nasledov, *Phys. Stat. Sol.*, **21**, 9, 1967.
- [31] S. C. Abrahams and J. L. Bernstein, *J. Chem. Phys.*, **61**, 1140, 1974.
- [32] H. J. Monkhorst and J. D. Pack, *Phys. Rev. B*, **13**, 5118, 1976.
- [33] J. E. Jaffe and A. Zunger. *Phys. Rev. B*, **29**, 1882, 1984.
- [34] V. Fiorentini and A. Baldereschi. *J. Phys. Condens. Matter*, **4**, 5967, 1992.
- [35] J. P. Poirier. In *Introduction to the Physics of the Earth's Interior*. Cambridge University Press, New York, 1991.
- [36] E. Francisco, J. M. Recio, M. A. Blanco, A. Martin Pendás, and A. Costales. *J. Phys. Chem. A*, **102**, 1595, 1998.
- [37] K. Böhmhammel, P. Deus, and H. A. Schneider. *Phys. Stat. Sol. (a)*, **65**, 563, 1981.
- [38] A. Shileika. *Surf. Sci.*, **73**, 730, 1974.
- [39] In ZnGeP_2 , the conduction band minimum and the valence band maximum is at Γ . Note that ZnGeP_2 has a binary analog GaP which has the

minimum of the conduction band at X. The X point of the zincblende structure corresponds to the Γ -point in the chalcopyrite Brillouin zone making the gap to be direct. A band gap of this nature is referred to as **pseudo-direct**.

[40] The pressure coefficients of valence and conduction levels are calculated from the variation of their energies with pressure.

[41] R. A. Bendorius, V. D. Prochukhan, and A. Shileika. *Phys. Stat. Sol. (b)*, **53**, 745, 1972.

[42] J. Fraxedas, L. Artus, and E. Paumier. *Jpn. J. Appl. Phys. Suppl.*, **32**, 503, 1993.

Table 1: Valence band energies in eV at Γ , T , N k-points in the Brillouin zone of CdGeAs₂.

Level	
As p band maxima	
Γ_{4v}	0.00
Γ_{5v}	-0.33
$T_{3v} + T_{4v}$	-1.26
N_{1v}	-0.72
As p band minima	
Γ_{4v}	-4.49
$T_{4v} + T_{5v}$	-3.86
N_{1v}	-5.06
Ge-As band	
Γ_{4v}	-7.05
Γ_{2v}	-9.44
T_{5v}	-7.50
N_{1v}	-7.52
Cd d band	
Γ_{max}	-8.24
Γ_{min}	-8.85
T_{max}	-8.40
T_{min}	-8.72
N_{max}	-8.50
N_{min}	-8.90
As s band	
Γ_{5v}	-11.04
Γ_{3v}	-11.09
Γ_{1v}	-13.10
$T_{1v} + T_{5v}$	-11.09
T_{5v}	-12.34
N_{1v}	-11.23
N_{1v}	-12.19

Table 2: The minimum-energy direct and pseudo-direct band gaps and crystal field splittings (in eV) for CdGeAs₂

	DFT gap	Corrected gap	Experiment
E_{direct}	0.16	0.98	0.61 ^a
$E_{pseudo-direct}$	1.16	1.98	--
Δ_{cf}	-0.33	--	-0.21

^a Ref. [7]

Table 3: Bulk moduli and related properties of CdGeAs₂

	B_0 (GPa)	B_S (GPa)	B'_0	B''_0 (GPa ⁻¹)
This work : 0K	57.03	57.03	4.79	-0.32
This work : 300K	53.21	54.43	5.47	-0.46
Experiment ^a : 300K	69.7	---	6.18	---

^a Ref. [13]

Table 4: Pressure coefficients in (10^{-6} eV/bar) of valence and conduction levels of CdGeAs₂.

<i>Level</i>	
Γ_{5v}	0.9
Γ_{4v}	6.5
Γ_{3c}	-2.9
Γ_{1c}	16
T_{3v+1v}	-0.87
T_{5c}	2.2
N_{1v}	2.6
N_{1c}	8.4

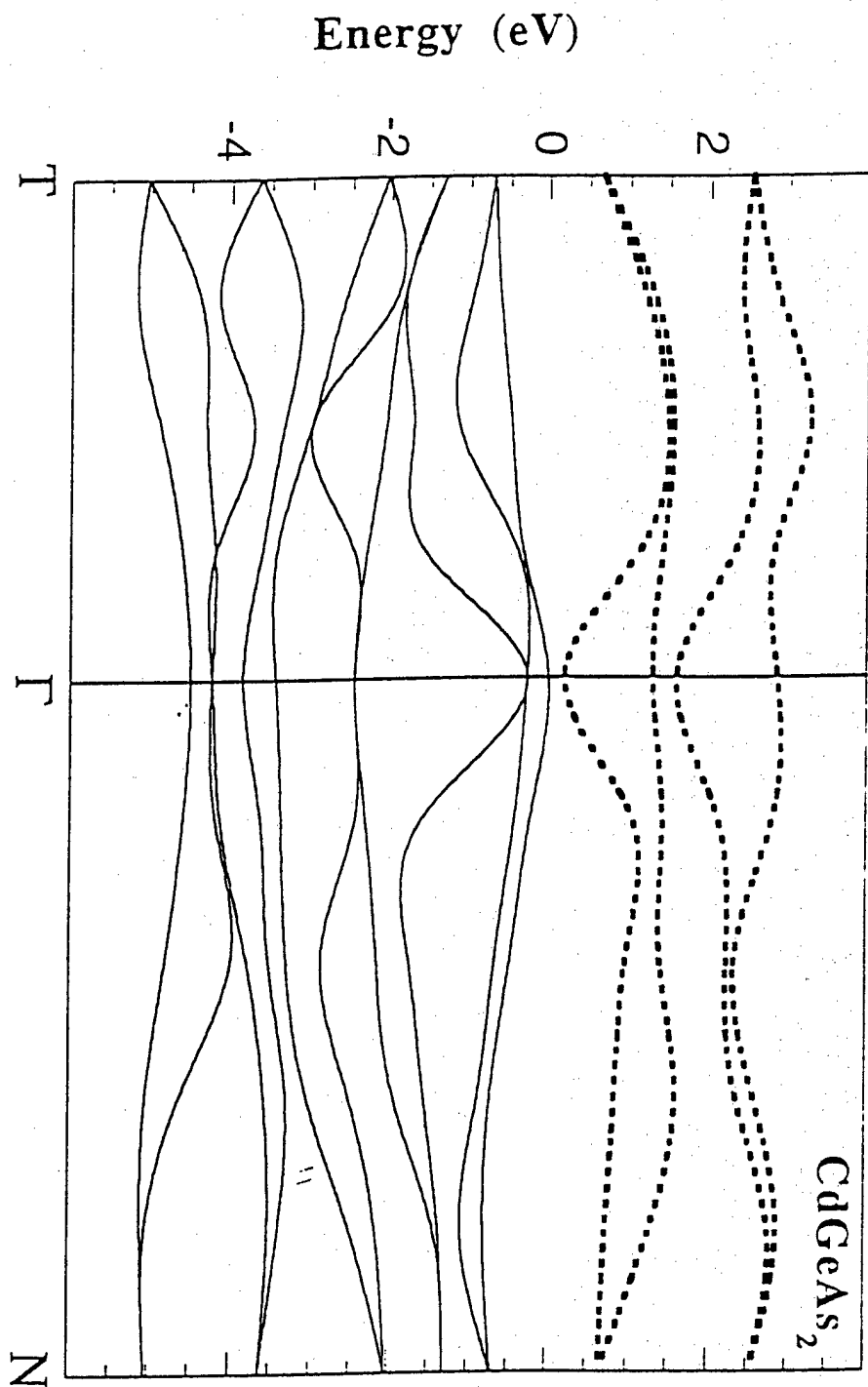
Figure Captions

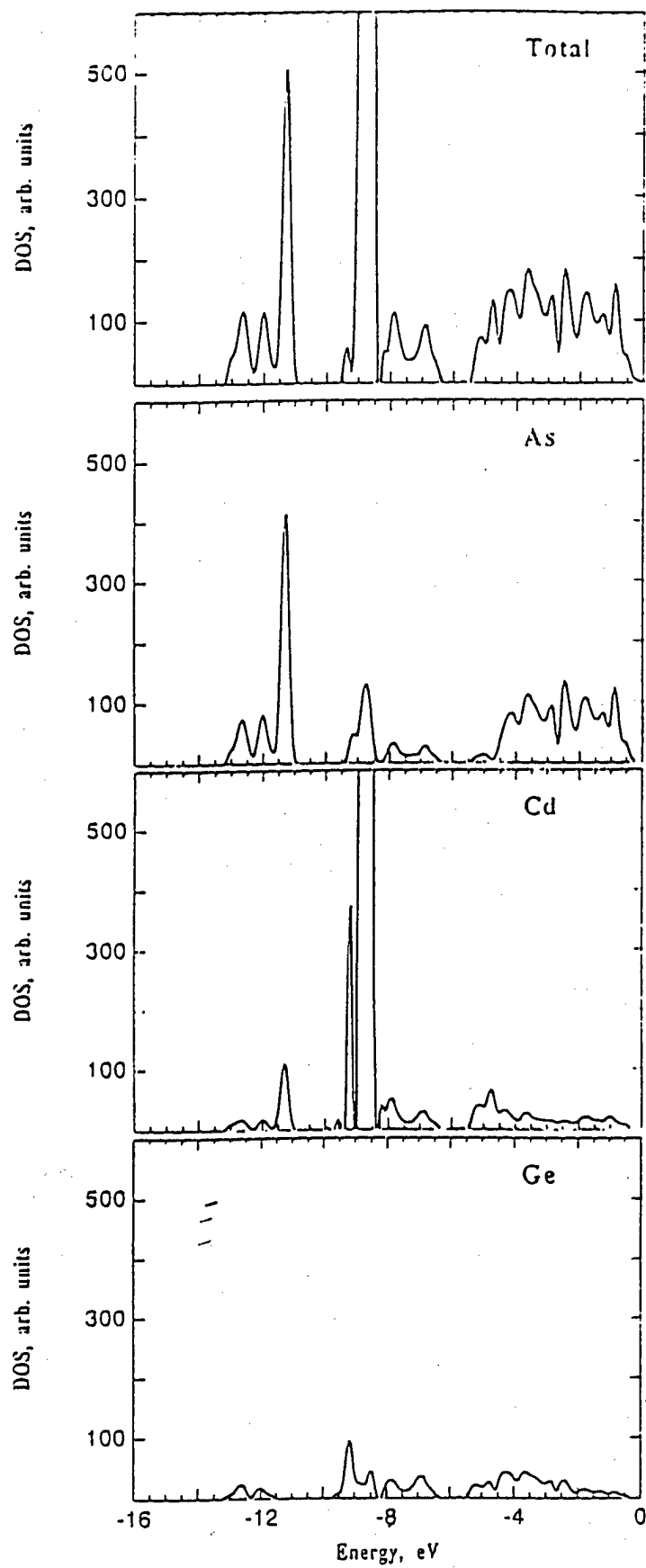
Fig. 1 : Electronic band structure of CdGeAs_2 .

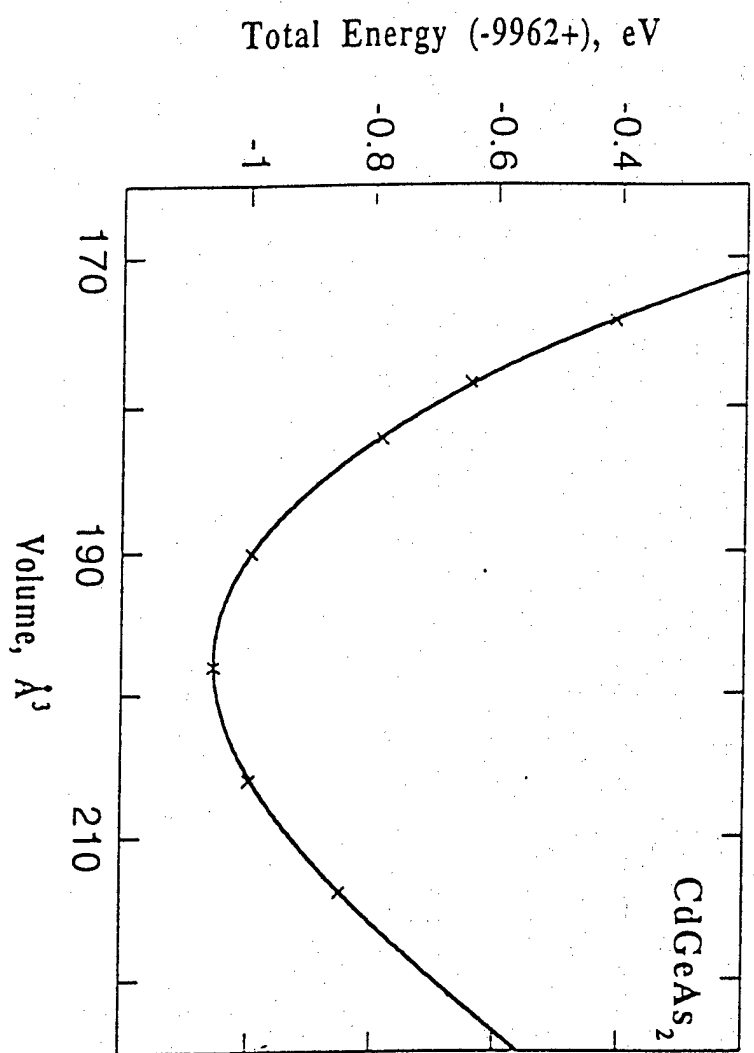
Fig. 2 : Total and Projected density of states of CdGeAs_2 .

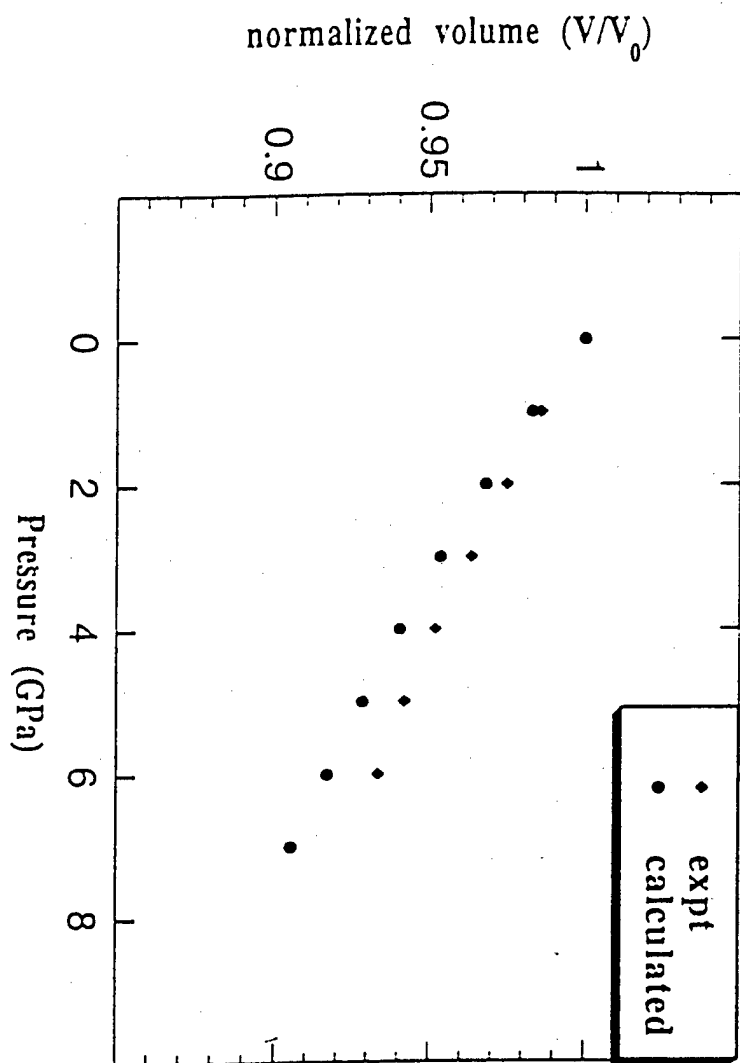
Fig. 3 : Total Energy vs volume of CdGeAs_2 in chalcopyrite phase.

Fig. 4 : Equation of State of CdGeAs_2 .









Atomistic Modeling of Native Defects in CdGeAs₂

I. INTRODUCTION :

Cadmium germanium arsenide (CdGeAs₂) is an important material due to its suitability for nonlinear optical applications in the infrared region since it has the highest nonlinear optical coefficient, 236 pm/V, known for a phase matchable compound semiconductor. Additionally, it has a wide transparency region extending across the infrared from 2.4 to 18 μm .¹⁻³ The availability of large single crystals⁴ of CdGeAs₂ has led to renewed efforts to utilize this material for frequency doubling (i.e., for second harmonic generation) carbon dioxide laser emission lines from 9.3 to 10.6 μm . The transparency of these crystals⁴, although superior to that of earlier crystals¹ is still limited by the photo-ionization of native acceptors.

Nominally undoped Bridgman grown single crystals of CdGeAs₂ are found to be p-type. Hall effect measurements^{5,6} on the best available crystals indicate the presence of a single acceptor with an activation energy of 0.15 eV. On the other hand, Brudni et. al.⁷, Halliburton et. al.⁸ and Smith et. al.⁹ utilizing respectively radiation damage techniques, EPR and thermal admittance spectroscopy measurements observe that there can be at least two native acceptors present in as-grown CdGeAs₂. Smith et. al.⁹ have found that there is a level with an activation energy of 0.11-0.13 eV in agreement with Hall measurement on the same samples, and a second deeper acceptor with an activation energy of 0.346 eV. It is the goal of this work to determine theoretically which native defects might give rise to these two acceptor centers in CdGeAs₂.

Theory has so far focused on calculating intrinsic properties such as the band structure^{10,11} and has not considered the chemistry of defects in this material. In this

paper, we perform such a task considering vacancies, interstitials and antisites in CdGeAs₂. We use atomistic simulation methods based on the shell model to describe the crystalline lattice of CdGeAs₂ and will calculate formation energies of native defects and binding energies of the acceptor centers. We note here that this approach has been very successful in yielding reliable defect energies in a wide variety of materials including sixfold- and fourfold-coordinated structures.¹² Recent applications of the shell model include structural relaxation around dopants in sapphire¹³, high-pressure phase transition in GaN¹⁴ and defect energetics in ZnGeP₂.¹⁵

II. PERFECT LATTICE

In the present atomistic description of a crystal, the lattice is considered to consist of ions interacting via a combination of electrostatics and interatomic potentials, while polarization is included by means of the shell model.¹⁶ The total energy of a crystal is then taken to be a sum of two- and three-body interactions in the lattice. The (two-body) pairwise interaction term consists of the long-range Coulombic part and the short-range repulsive part and is given by

$$E_{ij} = (Q_i Q_j / R_{ij}) + V_{SR}(R_{ij}), \quad (1)$$

where Q 's are charges and R_{ij} is the separation between ions. $V_{SR}(R_{ij})$ represents the short-range interaction between ions and is given by an analytical expression of the Born-Mayer form :

$$V_{SR}(R_{ij}) = A_{ij} \exp(-R_{ij} / \rho_{ij}), \quad (2)$$

where A and ρ are the parameters obtained generally by empirical fitting methods.

Three-body interaction terms in our model are represented by the Axilrod-Teller¹⁷ potentials:

$$E_{ijk} = k_{ijk} (1 + 3 \cos \theta_i \cos \theta_j \cos \theta_k) / R_i^3 R_j^3 R_k^3, \quad (3)$$

where k_{ijk} is a coefficient, θ_i is the i th angle and R_i is the side of the triangle formed by ions i, j and k in the lattice.

To describe the polarizability, we employ the shell model description of the lattice atoms. In the shell-model, each atom consists of a core of charge X , and a shell of charge Y , such that the total charge is the sum of the core and shell charges. The polarization is then simulated by the displacement of a shell from a core, the two being connected by a harmonic spring with a force constant K .

CdGeAs_2 crystallize in the chalcopyrite phase^{18,19} with a tetragonal symmetry group of $I4_2d$. Chalcopyrites can be constructed²⁰ by first considering a superlattice of the (cubic) zincblende phase with $c/a=2$, replacing each half of cations by Cd and Ge ions respectively and finally introducing a small distortion along z -axis leading to $c/a = 1.889$. As shown in Fig. 1, each atom is tetrahedrally coordinated in the lattice; cadmium or germanium cations have 4 near-neighbor arsenic anions while arsenic anions have 2 cadmium and 2 germanium cations as near-neighbors. In the lattice, cations occupy special positions labeled as a and b with no positional degrees of freedom, while anions are placed in the d positions given by the internal parameter, x . The value of x varies from crystal to crystal and is related to tetragonal distortion (i.e. $2 - c/a$) in the lattice. For CdGeAs_2 the lattice parameters¹⁹, a and c are 5.9432 Å and 11.2163 Å respectively at 298 K and the parameter x is 0.2785 leading to the interatomic distances of 2.629 Å for Cd-As and 2.430 Å for Ge-As.

In the chalcopyrite lattice, the tetrahedral coordination of atoms suggests that the covalent bonding (with sp^3 -hybrid bonds) predominates. On the other hand, the composition of the cation sublattice indicates a presence of the ionic character in the chemical bonding. In CdGeAs_2 a relatively large magnitude of tetragonal compression ($\approx 6\%$) confirms that the chemical bonding is mixed. Based on the electronegativities of the constituent atoms, the Ge-As bond is expected to be less ionic than the Cd-As bond. Our

atomistic model therefore do not assume either fully covalent (i.e. $\text{Cd}^{2+}\text{Ge}^0\text{As}_2^{1+}$) or fully ionic (i.e. $\text{Cd}^{2+}\text{Ge}^{4+}\text{As}_2^{3-}$) description of the lattice, but uses the empirical fitting method to determine the charges associated with Cd, Ge and As. Hence, the mixed (ionic-covalent) chemical bonding is taken into account by the use of the derived atomic charges along with the three-body terms included in the atomistic description of the material.

In our model, the two-body interaction term (Eq. 2) therefore requires the determination of Q_{Cd} , Q_{Ge} , Q_{As} and V_{SR} (i. e. parameters A and ρ) for the Cd-As, Ge-As and As-As interactions in CdGeAs_2 . Note that the short-range interactions between Cd-Cd and Ge-Ge are ignored as they become very small for large separations ($> 4.0 \text{ \AA}$) in the lattice. We also need to determine the coefficient k_{AsGeAs} and k_{AsCdAs} for the three-body terms (Eq. 3) along with the shell-model parameters Y_{As} and k_{As} . Both cations are considered as rigid ions in the lattice. All of these potential parameters are obtained by the empirical fitting method²¹ which uses the experimentally known crystal properties such as crystal structure^{18,19}, elastic²² and dielectric^{1,23} constants of CdGeAs_2 . Fitting and all calculations were performed using the program GULP.²⁴

Table I lists the model parameters representing the interatomic interactions in the lattice. The calculated crystal properties are compared with the experimental data in Table II. Accordingly, the potential model reproduces the lattice structure very well. The overall good agreement between the calculated and experimental properties for the perfect lattice indicates the reliability of the derived interatomic potential set for CdGeAs_2 .

III. NATIVE DEFECTS

Defect energies of several plausible types of ionic and electronic native acceptor defects have been calculated using the Mott-Littleton methodology^{25,26} in which the lattice is divided into a series of different regions around the defect by concentric spherical boundaries. Immediately surrounding the defect is region 1 in which all ions are treated

explicitly and fully optimised. Beyond this is region 2a in which all atoms are still explicitly considered, but the relaxation effects are much smaller and can be treated more approximately. The validity of the successive approximations made in the above multiregion method improves as the radii of the regions increase. Therefore it is important to check the convergence of the results with region size. In the present work a region 1 containing approximately 350 atoms was found to be sufficient to converge the absolute defect energy to better than 0.01 eV, though relative energies will be far more converged than this. We also note here that provide the defects are charge neutral overall and the quality of fitting to the structural properties are the same, then to the first order the defect energies should not depend too strongly on the charges used in the model. If defect-induced displacements in the lattice are large then the particular shape of the anharmonic region of the potential energy curve will become more important thereby yielding a strong dependence of defect energies on the charges. However, given that we know the ions in CdGeAs_2 do not have integral charges, the use of partial charges is therefore expected to give a better account of this anharmonic region in defect calculations.

The Schottky defects in the lattice are formed by moving the constituent ions to the surface from their bulk sites whereas the Frenkel defects are pairs of the vacancy and interstitial of the same type of ion. In calculations an interstitial was simulated as an addition of atom to the empty interstitial position in the lattice. The Schottky, Frenkel and antisite formation energies (Table III) were obtained from defect energy calculations of vacancies, interstitials and antisites in the lattice. In CdGeAs_2 the Schottky defect is $(V_{\text{Cd}}+V_{\text{Ge}}+2V_{\text{As}})$, the Frenkel defect pairs are $(V_{\text{Cd}}+\text{Cd}_i)$, $(V_{\text{Ge}}+\text{Ge}_i)$ and $(V_{\text{As}}+\text{As}_i)$ and the antisite pairs are $(\text{Cd}_{\text{Ge}}+\text{Ge}_{\text{Cd}})$, $(\text{Cd}_{\text{As}}+\text{As}_{\text{Cd}})$ and $(\text{Ge}_{\text{As}}+\text{As}_{\text{Ge}})$. As shown in Table III, the lowest formation energy comes out to be for the $(\text{Cd}_{\text{Ge}}+\text{Ge}_{\text{Cd}})$ antisite pair which is followed by the Schottky and Frenkel pairs of Cd and Ge. The large formation energies for the antisite pairs, $(\text{Cd}_{\text{As}}+\text{As}_{\text{Cd}})$ and $(\text{Ge}_{\text{As}}+\text{As}_{\text{Ge}})$, would seem to preclude their occurrence

as intrinsic point defects in CdGeAs_2 . This ordering of formation energy is what we expected since the magnitude of formation energy depends mainly on the extent of distortion introduced by individual defects in the lattice. In the present case, antisite disorder in the cation sublattice introduces least distortion in the lattice compared to that introduced by either vacancies, interstitials and antisites involving both cation and anion sublattices.^a We note here that (tetrahedral) covalent radii of Cd, Ge and As ions are 1.405, 1.225 and 1.225 Å respectively ²⁷.

The magnitude of the formation energy for the $(\text{Cd}_{\text{Ge}} + \text{Ge}_{\text{Cd}})$ antisites is small (≈ 0.3 eV) suggesting that appreciable disorder would occur in the cation sublattice at higher temperatures. This is in accord with what has been reported for CdGeAs_2 which has a high-temperature disordered zincblende phase. In this phase, Cd and Ge occupy cation sites randomly in contrast to the ordered chalcopyrite phase where Cd and Ge occupy alternating cation sites. Upon cooling to room temperature, the lattice is then expected to retain some of the disorder in the cation sublattice.

IV. NATIVE ACCEPTORS :

A native acceptor center in CdGeAs_2 may involve either cation vacancy (V_{Cd} or V_{Ge}) or antisite (Cd_{Ge}) based on the effective charge considerations and can stabilize a hole on near-neighbor As ions with the binding energy given by :

$$\Delta E = E_A + E_h - E_{h+A} \quad (4)$$

where E_{h+A} refers to energy of the hole-acceptor complex, E_h is energy of the hole and E_A is energy of the acceptor in the lattice. For the bound hole, ΔE is taken to be positive.

The hole-acceptor complex in CdGeAs_2 can be classified according to the degree of delocalization of the hole states in the lattice. For example, a complete delocalization refers

^a a detailed list of individual defect energies and lattice coordinates can be obtained from the authors (pandey@mtu.edu)

to sharing of a hole by all of the four As neighbors of the acceptor (i.e. 4-center case). Alternatively, a hole next to the acceptor center may be shared by a pair of As neighbors (i.e. 2-center case) or localized on one of the As ions (i.e. 1-center case) in the lattice. The presence of hole-acceptor complexes in as-grown CdGeAs₂ has been revealed by Hall-effect measurements^{5,6,28}, electron paramagnetic resonance (EPR)⁸, and thermal admittance spectroscopy.⁹ We note here that a direct comparison can be made between ΔE and the acceptor binding energy obtained from the Hall-effect measurements.

Our approach to calculation of ΔE is similar to that used in an earlier study¹⁵ of ZnGeP₂ where we assumed that the presence of a hole in the lattice reduces the (shell) charge thereby only modifying long-range Coulombic interactions between ions. The short-range interaction parameters (Eq. 2) are taken to be the same as obtained for the perfect lattice. This assumption is likely to overestimate the 1-center hole binding energy slightly since it provides a more accurate treatment of the delocalized hole (4-center case) relative to the localized hole (1-center case). Furthermore, we expect, to a first approximation, cancellation of the hole self-interaction energies in Eq. 4 for the 4-center case since ΔE is the difference of two terms involving the delocalized hole.

Calculations based on the Mott-Littleton methodology (described in Sec. III) are performed to obtain defect energies for eq. 4 to calculate ΔE . These include, for example, antisite (E_A), delocalized hole (E_h) and antisite next to the delocalized hole (E_{h+A}) in the lattice. All defect coordinates are fully optimized in these calculations. The calculated binding energies (ΔE) are given in Table IV. Accordingly, a striking distinction is found in the binding energies of acceptors associated with either vacancies or antisites for different hole localization regions. The hole tends to be localized near a cation vacancy, i.e., the more the hole is localized, the larger is the binding energy. But the trend is exactly opposite for antisites where a larger binding energy is found to be associated with the delocalized hole. It is well known that the localization of a hole in the lattice is a result of interplay

between lattice distortion and polarization. In CdGeAs_2 , the distinct behavior of hole localization can therefore be understood in terms of the distortion and polarization introduced by these defects in the surrounding lattice. For example, a V_{Cd} has an effective charge of $-1.8e$ in comparison to the effective charge of $-0.5e$ associated with Cd_{Ge} . The difference in effective charges along with the fact that a Cd atom is much larger than the Ge atom results in an inward relaxation ($\approx 6\%$) of As neighbors for V_{Cd} in contrast to an outward relaxation ($\approx 5\%$) of As neighbors for Cd_{Ge} . Based on simple electrostatic arguments, the localized hole (i.e. 1-center case) is therefore expected to have a larger binding energy for V_{Cd} than that for Cd_{Ge} .

As shown in Table IV the calculated binding energies for various acceptor centers vary from 0.04 to 0.80 eV. Note that the energy gap for this material is only 0.57 eV at room temperature. For Hall effect measurements on the best available crystals^{5,6}, a value of 0.15 eV is obtained for the acceptor binding energy. The acceptor center revealed in the Hall-effect measurements is therefore likely to be associated with the delocalized hole (i.e. 4-center case) in the vicinity of Cd_{Ge} for which calculations yield the binding energy of about 0.13 eV. The acceptor center involving V_{Cd} was not chosen as one would expect the deepest level, 0.49 eV, to be its populated level (Table IV). We note here that a detailed electronic structure study of these defect-complexes is planned to confirm the proposed assignment of the acceptor centers in CdGeAs_2 .

In fact, our prediction regarding the nature of the dominant acceptors is confirmed by the EPR measurements. Halliburton et al.⁸ have proposed that the dominant EPR signal may be due to the acceptor center consisting of either a cation vacancy or antisite cation with the unpaired spin shared by the four neighboring As ions. This is consistent with our selection of the shallow acceptor as the cation antisite, Cd_{Ge} . Our further analysis of the calculated results find that the near-neighbors of V_{Cd} relax inward by 0.08 Å in contrast to the outward relaxation of near-neighbors of Cd_{Ge} of about 0.19 Å from their regular

lattice sites (Table V). It is to be noted here that the magnitude of the lattice distortion introduced by acceptors can be used in the analysis of (future) magnetic resonance studies to ascertain more precisely the nature of the EPR-active center.

Recent capacitance-voltage measurements using thermal admittance spectroscopy⁹ have reported the presence of two acceptor levels in p-CdGeAs₂ with binding energies of 0.11-0.13 eV and of 0.346 eV. The first acceptor level is the same one revealed by Hall effect measurements yielding binding energies of 0.10 - 0.12 eV for these exact same samples⁵ which are fairly heavily doped. This value corresponds to the delocalized hole (i.e. 4-center case) bound to the Cd_{Ge} as previously discussed. Based on comparison of the binding energy of the second acceptor with the calculated binding energies (Table V), we predict that the deeper acceptor is associated with the localized hole bound to V_{Cd}, as this center's deepest level will be populated. The other possibilities can be ruled out as they have binding energies which exceed the band gap of CdGeAs₂.

5. SUMMARY

A set of interatomic potentials consisting of two- and three-body potential parameters coupled with the shell model description of the lattice is developed for CdGeAs₂ reproducing its structural, elastic and dielectric properties successfully. Native defect formation energies show that antisites in the cation sublattice will dominate the intrinsic disorder in this material. The dominant acceptor center controlling the optical properties of this material and revealed in the EPR and Hall-effect measurements is likely to be a hole shared by four neighboring As ions in the vicinity of Cd_{Ge}. The deeper level is probably due to a hole localized on one As ion and bound to V_{Cd}.

Although ZnGeP₂ and CdGeAs₂ belong to the same chalcopyrite family, the nature of dominant acceptors in these materials is predicted to be different. Defect calculations corroborating the Hall effect and magnetic resonance studies find that the zinc vacancy, not

the zinc antisite (Zn_{Ge}), is associated with the dominant acceptor center in ZnGeP_2 . This is not the case in CdGeAs_2 where a cadmium antisite (Cd_{Ge}) is predicted to be associated with the dominant acceptor in the lattice. We believe that this difference may well be due to defect-induced lattice distortion which plays a key role in stabilizing the hole states in the lattice. Based on the size argument, native acceptors associated with zinc antisites (Zn_{Ge}) are not expected to introduce significant lattice distortion in ZnGeP_2 since both Zn and Ge have the same tetrahedral radius²⁷ of 1.23 Å. On the other hand, the tetrahedral radius of Cd is about 1.41 Å. Therefore, the size difference of about 15% between Cd and Ge would be expected to cause significant distortion by a cadmium antisite (Cd_{Ge}) in the CdGeAs_2 lattice.

References :

- ¹ R. L. Byer, H. Kildal, and R. S. Feigelson, Appl. Phys. Lett. 19, 237 (1971); H. Kildal, AFML-TR-72-277 (Government technical report available from NTIS, #AD739556), 1972.
- ² G. D. Boyd, E. Buehler, F. Storz, and J. H. Wernick, IEEE J. Quantum Electron. QE-8, 419 (1972).
- ³ V. G. Dmitriev, G. G. Gurzadayan, and D. N. Nikogosyan, *Handbook of Nonlinear Optical Crystals*, (Springer-Verlag, New York, Berlin, Heidelberg, 1991 & 1997 for Revised Edition).
- ⁴ P. G. Schunemann, in *OSA Conference on Lasers and Electro-Optics, Vol. 9, OSA Technical Digest Series* (Optical Society of America, Washington, DC), 1997.
- ⁵ D. W. Fischer, M. C. Ohmer and J. E. McCrae, J. Appl. Phys. 81, 3579 (1997).
- ⁶ V. Yu. Rud and Yu. V. Rud, Jpn. J. Appl. Phys., Suppl. 32.3, 672 (1993).
- ⁷ V. N. Brudnyi, M. A. Krivov, A. I. Potapov, IO. K. Polushina, V. D. Prochukhan, Yu. V. Run, Phys. Stat. Sol. (a) 49, 761 (1978).
- ⁸ L. E. Halliburton, G. J. Edwards, P. G. Schunemann and T. M. Pollak, J. Appl. Phys. 77, 435 (1994).
- ⁹ S. R. Smith, A. O. Evwaraye and M. C. Ohmer, MRS Fall Meeting Fall 1997.

- 10 R. Madelon, E. Paumier and A. Hairic, *Phys Stat. Sol. (b)* **165**, 435 (1991).
- 11 P. Zapol, R. Pandey and M. C. Ohmer, MRS Fall Meeting-Abstract O7.8, 1996.
- 12 J. H. Harding and A. M. Stoneham, *J. Phys. C* **15**, 4649 (1982).
- 13 P. Kizler, J. He, D. R. Clarke and P. R. Kenway, *J. Am. Ceram. Soc.* **79**, 3 (1996).
- 14 P. Zapol, R. Pandey and J. D. Gale, 1997, submitted for publication.
- 15 P. Zapol, R. Pandey, M. Ohmer, and J. D. Gale, *J. Appl. Phys.* **79**, 671 (1996).
- 16 B. G. Dick and A. W. Overhauser, *Phys. Rev.* **112**, 90 (1958).
- 17 B. M. Axilrod and E. Teller, *J. Chem. Phys.* **11**, 299 (1943).
- 18 A. S. Borshchevskii, N. A. Goryunova, F. P. Kesamanly and D. N. Nasledov,
Phys. Stat. Sol. **21**, 9 (1967).
- 19 S. C. Abrahams and J. L. Bernstein, *J. Chem. Phys.* **61**, 1140 (1974).
- 20 J. L. Shay and J. H. Wernick, *Ternary Chalcopyrite Semiconductors: Growth, Electronic Properties, and Applications* (Pergamon, New York, 1975).
- 21 J. D. Gale, *Phil. Mag.* **B73**, 3 (1996).
- 22 T. Hailing, G. A. Saunders, W. A. Lambson and R. S. Feigelson, *J. Phys. C* **15**, 1399 (1982).
- 23 L. Artus, J. Pascual and J. Camassel, *Materials Sci and Engng.* **B5**, 239 (1990).
- 24 J. D. Gale, *JCS Faraday Trans* **93**, 629 (1997).
- 25 A. B. Lidiard and M. J. Norgett in *Computational Solid State Physics*, edited by F. Herman (Plenum, New York, 1972), p. 385.
- 26 C. R. A. Catlow and W. C. Mackrodt, *Computer Simulations of Solids* (Springer, Berlin, 1982).
- 27 J. A. Van Vechten and J. C. Phillips, *Phys. Rev. B* **2**, 2160 (1970).
- 28 G. W. Iseler, H. Kildal, and N. Menyuk, *J. Electron. Mater.* **7**, 737 (1978).

TABLE I. Interatomic potential parameters of Eqs. 2 and 3. The atomic charges are +1.83e, +2.29e and -2.06e for Cd, Ge and As, respectively. For As, the shell charge (Y) is -2.22e and the spring constant (K) is 1.40 eVÅ⁻².

	A_{ij} (eV)	ρ_{ij} (Å)	k_{ijk} (eVÅ ⁻⁹)
Cd - As	329.5	0.4826	
Ge - As	531.6	0.4119	
As - As	32228.9	0.3131	
Cd-As-As			272.4
Ge-As-As			-277.5

TABLE II. Calculated and Experimental bulk properties of CdGeAs₂.

		This work	Experiment
Structure	a , Å	5.951	5.9432 ^a
	c , Å	11.221	11.2163
	c/a	1.886	1.887
	x_{As}	0.279	0.2785
Lattice energy/unit cell, eV			
	E_L	-134.6	---
Elastic constants (10^{11} dyn cm ⁻²)			
	C_{11}	9.70	9.45 ^b
	C_{12}	4.47	5.96
	C_{13}	5.45	5.97
	C_{33}	8.95	8.34
	C_{44}	4.26	4.21
	C_{66}	3.42	4.08
Dielectric constants			
	ϵ_0^{11}	14.75	14.8 ^c
	ϵ_0^{33}	15.43	15.4
	ϵ_∞^{11}	10.17	10.06 ^d
	ϵ_∞^{33}	10.93	11.04

(a) reference 19 (b) reference 22 (c) reference 23 (d) reference 1

TABLE III. Native defect formation energies in CdGeAs₂.

Formation energy (per defect), eV	
Schottky pair :	
(V _{Cd} +V _{Ge} +2V _{As})	1.88
Frenkel pair :	
(V _{Cd} +Cd _i)	2.39
(V _{Ge} +Ge _i)	2.82
(V _{As} +As _i)	5.07
Antisite pair :	
(Cd _{Ge} +Ge _{Cd})	0.28
(Cd _{As} +As _{Cd})	12.1
(Ge _{As} +As _{Ge})	13.1

TABLE IV. The calculated binding energies (ΔE of eq. 4) of native acceptors in CdGeAs_2 .

Acceptor center ^a	1-center	2-center	4-center
Hole near V_{Cd}	0.49 eV	0.26 eV	0.15 eV
Hole near V_{Ge}	0.80	0.67	0.59
Hole near Cd_{Ge}	0.04	0.12	0.13

^aLocalization of a hole on a As, two As and four As neighbors to the cation site is represented by 1-center, 2-center and 4-center cases respectively.

TABLE V. The calculated lattice distortion introduced by native acceptors in CdGeAs_2 .

Acceptor center	Near-neighbor Separation ^a , Å		
	1-center	2-center	4-center
Hole near V_{Cd}	2.38	2.50	2.56
Hole near V_{Ge}	2.26	2.37	2.41
Hole near Cd_{Ge}	2.97	2.71	2.62

^a The near-neighbor separations in the perfect lattice are 2.43 and 2.63 Å for Ge-As and Cd-As, respectively.

Atomistic Calculations of Dopant Binding Energies in ZnGeP₂

INTRODUCTION

Zinc germanium phosphide (ZnGeP₂) is the NLO material for mid IR lasers allowing high-power tunability in the spectral region of 2-5 μm .¹⁻² An absorption band around 1-2 μm is, however, found to affect the usefulness of this material. This band is attributed to photoionization of a deep native acceptor center associated with the zinc vacancy.³⁻⁵ Experimental efforts involving selective doping of the material are underway to reduce the concentration of this acceptor-complex in the lattice. Earlier work on the properties of dopants in ZnGeP₂ have been limited to few photoluminescence and Hall effect studies. Averkieva et al. have reported⁶ photoluminescence spectra and hole concentrations for crystals melt doped with Cu, Ga, In, Se, Fe, Cd and Si. The room temperature hole concentration for these samples were reported to vary from a low of $2.8 \times 10^{10}/\text{cm}^3$ for Si, nominally the value seen in undoped crystals, to a high of $10^{17}/\text{cm}^3$ for In. Based on a photoluminescence study⁷, it is reported that Cu diffusion can increase the hole concentration by a factor of 10,000 in ZnGeP₂ by a proper choice of the diffusion regime. Grigoreva et al., however, have reported⁸ Hall effect data on samples doped with Au, Cu, Se, Ga and In and stated that the first two dopants were inactive and the rest were acceptors. The binding energy of Se was reported to be 0.40 eV and that of Ga to be 0.30 eV. In a more recent review paper, Rud⁹ has indicated that Au, Cu, Ga, In, Se and Pt are acceptors with activation energies in eV of respectively 0.50, 0.30, 0.06 for heavy doping, 0.03 for heavy doping and ≈ 0.4 for light doping, 0.40 and 0.50. These results will be compared with our calculated values later in the paper.

We have initiated an extensive theoretical study⁵ on ZnGeP₂ and, in this paper, we will report the results of atomistic calculations involving cation dopants, namely Cu, Ag, B, Al, Ga and In. The choice of dopants is expected to indicate the ion-size effect on the binding energies for the groups I and III dopants which lie left and right columns of the host Zn ion in the periodic table. Our approach is based on the pair-wise description of the lattice which has been very successful in yielding reliable defect energies in a wide variety of materials including sixfold- and fourfold-coordinated structures.¹⁰⁻¹¹

INTERATOMIC POTENTIALS

In our approach, the lattice is considered to consist of ions interacting via a combination of electrostatics and interatomic potentials, while polarization is included by means of the shell model.¹² The total energy of a crystal is then taken to be a sum of two-body interactions in the lattice. The pairwise interaction term consists of the long-range Coulombic part and the short-range repulsive part which is given by an analytical expression of the Born-Mayer form :

$$V_{SR}(R_{ij}) = A_{ij} \exp(-R_{ij}/\rho_{ij}), \quad (1)$$

where A and ρ are the parameters yet to be determined.

We apply a parameter-free procedure to model interatomic interactions of dopant ions with the host P^{3-} anion. The general strategy has been described in detail previously¹⁰ and consist of two steps : (i) generation of quantum-mechanical crystalline ionic electronic densities (IEDs) for the ions involved in the interaction, and (ii) application of the electron gas formalism¹³ to derive the corresponding crystal consistent interatomic potential (CCIP). To obtain the quantum-mechanical description of P^{3-} embedded in the $ZnGeP_2$ environment, we have used the ab-initio Perturbed Ion (aiPI) model.¹⁴ The minimization of the total crystal energy required by the Hartree-Fock approach provides a set of crystal-like atomic wavefunctions that respond self-consistently to the nearly exact crystal potential. In our case the aiPI computation has been performed at the experimental value of the lattice parameters of $ZnGeP_2$ using the Slater type orbitals given by Clementi and Roetti.¹⁵ It is interesting to remark that the essential electron gas assumption of the total crystal density being a superposition of the individual IEDs is better satisfied by the aiPI crystal-like orbitals than by solutions employed in earlier electron gas calculations. This behavior is mainly due to the inclusion in the representation of the aiPI crystal potential of a projection operator that enforces the ion-lattice orthogonality.

For calculations based on the electron gas theory, we have used the following functional forms to evaluate the pairwise interatomic energy : Thomas-Fermi for kinetic, Lee-Lee-Parr for exchange and Wigner (with the new fitting by Clementi) for correlation. The coulombic contributions has been exactly evaluated by means of analytical algorithms recently developed.^{16,17} To compute the rest of the contributions, we have used a

spheriodal(ϕ, λ, μ) coordinate system. The angular integration over ϕ is trivially 2π , since the electron density is cylindrically symmetric along the internuclear axis. In the cases of λ and μ , we have used a 60x60 Gauss-Legendre quadrature. The total volume of integration contains at least 99.9998% of the electron density. For each set of interatomic potential representing interaction between dopant and the P ion, the interatomic energy is evaluated at separations starting from 2 bohr to 12 bohr at intervals of 0.1 bohr.

The calculated potential energy surface for all the dopants considered here is shown in Fig. 1. The effect of ion-size is clearly illustrated here; higher the atomic number of a dopant, stronger its short-range interatomic interaction with P in the lattice. The energy surface is then fitted to the analytical expression (Eq. 1) whose parameters (i.e. A and ρ) are listed in Table I. For the host lattice, the interatomic potential parameters (i.e. Zn-P, Ge-P, P-P, Zn-Zn, Ge-Ge and Zn-Ge) along with the shell-model parameters Y_P and k_P parameters are obtained by the empirical fitting using the program GULP.¹⁹ Both dopant and host lattice cations are considered as rigid ions in the lattice. The derived interatomic potential set (Table I) for the host lattice reproduces the calculated crystal properties such as structure, elastic and dielectric constants very well.²⁰

DOPANT ENERGETICS

The nature of a cation dopant in ZnGeP_2 depends on the host atom which it is replacing in the lattice. In the present case, the group III dopants (i.e. B, Al, Ga and In) would either act as a donor substituting Zn or act as an acceptor when they replace Ge. The group I cations (i.e. Cu and Ag) would always be acceptors substituting either Zn or Ge in the lattice. The binding energy of an electron or a hole to the dopant can then be written as :

$$\Delta E = E_{\text{dop+iso}} - (E_{\text{iso}} + E_{\text{dop}}) \quad (2)$$

where $E_{\text{dop+iso}}$ refers to energy of the dopant complex, E_{iso} is energy of an isolated hole or electron and E_{dop} is energy of the dopant in the lattice. Calculations to obtain energies for Eq. 2 include, for example, Cu at the Zn site (E_{dop}), an isolated hole localized over As ions (E_c) and Cu next to the localized hole ($E_{\text{dop+c}}$) in the lattice. Note that a direct comparison can be made between ΔE and the acceptor binding energy obtained from the Hall-effect measurements.

Total energies of defects including both native and dopants have been calculated using the Mott-Littleton methodology^{21,22} in which the lattice is divided into a series of different regions around the defect by concentric spherical boundaries. Immediately surrounding the defect is region 1 in which all ions are treated explicitly and fully optimized. Beyond this is region 2a in which all atoms are still explicitly considered, but the relaxation effects are much smaller and can be treated more approximately. The displacements in region 2a can be calculated based on the force due to region 1. Beyond region 2a is region 2b in which the relaxation energy is treated yet more approximately and responds only to the total charge on the defect position at the defect center. Hence this component can be summed to infinity through the use of lattice summation methods analogous to the Ewald sum for the first inverse power of distance. In the present work, region 1 contains approximately 350 atoms which was found to be sufficient to converge the absolute defect energy to better than 0.01 eV.

The calculated binding energies (ΔE) for various dopants are given in Table II. At the Zn site in ZnGeP_2 , Cu and Ag acting as acceptors are predicted to have the binding energy of 0.25 and 0.17 eV respectively. Comparison of the calculated value with the experimental value of 0.30 eV for Cu shows a very good agreement. The group III dopants, on the other hand, have a donor-like nature at the Zn site. Their electron binding energies vary from 0.36 to 1.50 eV with a significant change in energy going from B to Al. This may be due to a large mismatch between the atomic sizes of B and Zn in the lattice (Table II). For Al, Ga and In, calculations yield large binding energies for the electron placing the donor levels in the middle of the gap in ZnGeP_2 . At the Ge site where the group III dopants act as acceptors, the results find a distinct behavior by B which forms a deeper center as compared to other ions. This difference can again be understood in terms of the large lattice relaxations arising due to difference in covalent radii of B and Ge which tend to stabilize the hole more strongly. The group I dopants (i.e. Cu and Ag) at the Ge site have a very large hole binding energy due mainly to electrostatic interactions, for example, between $[\text{CuGe}]^{\bullet\bullet}$ and a hole.

In summary, we have derived the interatomic potentials for various cation dopants in ZnGeP_2 and have calculated their binding energies to a hole or an electron depending on the substitution site in the lattice. The calculations based on atomistic description of the lattice predict that the group-III dopants would bind the hole more strongly than the

group-I dopants. Furthermore, the results find that dopants acting as donors introduce midgap states in ZnGeP_2 .

REFERENCES

- ¹ P. G. Schunemann, P. A. Budni, M. G. Knights, T. M. Pollok, E. P. Chicklis, and C. L. Marquardt, *Advanced Solid State Lasers and compact Blue-Green Laser Technical Digest* (Optical Society of America, Washington, DC, 1993).
- ² Yu. V. Rud, *Fiz. Techn. Poluprovodn*, 28 633 (1994).
- ³ M. H. Rakowsky, W. K. Kuhn, W. J. Lauderdale, L. E. Halliburton, G. J. Edwards, M. P. Scripsick, P. G. Schunemann, T. M. Pollak, M. C. Ohmer and F. K. Hopkins, *Appl. Phys. Lett.* 64, 1615 (1994).
- ⁴ L. E. Halliburton, G. J. Edwards, M. P. Scripsick, M. H. Rakowsky, P. G. Schunemann, and T. M. Pollak, *Appl. Phys. Lett.* 66, 2670 (1995).
- ⁵ P. Zapol, R. Pandey, M. Ohmer, and J. D. Gale, *J. Appl. Phys.* 79, 671 (1996).
- ⁶ G. K. Averkieva, V. S. Grigoreva, I. A. Maltseva, V. D. Prochukan, Yu. V. Rud, *Phys. Stat. Sol. (a)* 39, 453 (1977).
- ⁷ V. G. Voevodin, A. I. Gribenyukov, A. . Morozov and V. S. Morozov, *Izve Vys. Ucheb. Zav., Fiz* 2, 64, 1985.
- ⁸ V. S. Grigoreva, V. D. Prochukhan, Yu. V. Rud, A. A. Yakovenko, *Phys. Stat. Sol. (a)* 17, K69 (1973).
- ⁹ *Physical Phenomena in Ternary Compounds and Devices* by Yu. V. Rud (in Russian), Machine Translation-NAIC-ID(RS)T-0699-94, Distribution limited, available from DTIC.
- ¹⁰ J. H. Harding and A. M. Stoneham, *J. Phys.* C15, 4649 (1982).
- ¹¹ P. Zapol, R. Pandey and J. D. Gale, 1997, *J. Condens. Matter*, in press, 1997.
- ¹² B. G. Dick and A. W. Overhauser, *Phys. Rev.* 112, 90 (1958).
- ¹³ E. Francisco, J. M. Recio, M. A. Blanco, A. Martin Pendas and L. Pueyo, *Phys. Rev. B* 51, 2703 (1995).
- ¹⁴ R. G. Gordon and Y. S. Kim, *J. Chem. Phys.* 56, 3122 (1972).
- ¹⁵ V. Luana and L. Pueyo, *Phys. Rev. B* 41, 3800 (1990).
- ¹⁶ E. Clementi and C. Roetti, *At. Nucl. Data Tables* 14, 177 (1974).
- ¹⁷ E. Francisco, J. M. Recio, M. A. Blanco and A. Martin Pendas, *Phys. Rev. B* 51, 11289 (1995).
- ¹⁸ A. Martin Pendas and E. Francisco, *Phys. Rev.* A43, 3384 (1991).
- ¹⁹ J. D. Gale, *Phil. Mag.* B73, 3 (1996); J. D. Gale, *JCS Faraday Trans* 93, 629 (1997).

- ²⁰ A detailed comparison can be obtained from the authors : pandey@mtu.edu
- ²¹ A. B. Lidiard and M. J. Norgett in Computational Solid State Physics, edited by F. Herman (Plenum, New York, 1972), p. 385.
- ²² C. R. A. Catlow and W. C. Mackrodt, *Computer Simulations of Solids* (Springer, Berlin, 1982).

TABLE I. Interatomic potential parameters (given in Eq. 2) both for dopants (obtained by electron-gas methods) and the host lattice (obtained by empirical fitting method).

=====		
	A_{ij} (eV)	ρ_{ij} (Å)

electron-gas : $\text{Cu}^{1+} - \text{P}^{3-}$	1562.56	0.3694
$\text{Ag}^{1+} - \text{P}^{3-}$	2170.20	0.3514
$\text{B}^{3+} - \text{P}^{3-}$	2566.54	0.2808
$\text{Al}^{3+} - \text{P}^{3-}$	2310.8	0.3233
$\text{Ga}^{3+} - \text{P}^{3-}$	2567.12	0.3474
$\text{In}^{3+} - \text{P}^{3-}$	2879.71	0.3501
empirical : $\text{Zn}^{2+} - \text{P}^{3-}$	2776.92	0.2946
$\text{Ge}^{4+} - \text{P}^{3-}$	1030.93	0.4659
$\text{Zn}^{2+} - \text{Zn}^{2+}$	2776.92	0.2946
$\text{Ge}^{4+} - \text{Ge}^{4+}$	646.280	0.1996
$\text{Zn}^{2+} - \text{Ge}^{4+}$	23944.3	0.3406
$\text{P}^{3-} - \text{P}^{3-}$	1422.15	0.4932
=====		

TABLE II: Binding energies for various cation dopants in ZnGeP₂.

Dopant	Nature	Binding energy* (eV)	R _{dopant} ** (Å)
[Cu _{Zn}]	acceptor	0.25	1.35
[Ag _{Zn}]	acceptor	0.17	1.53
[B _{Zn}]	donor	0.36	0.88
[Al _{Zn}]	donor	1.05	1.26
[Ga _{Zn}]	donor	1.40	1.26
[In _{Zn}]	donor	1.49	1.44
[Cu _{Ge}]	acceptor	2.2	1.35
[Ag _{Ge}]	acceptor	2.0	1.53
[B _{Ge}]	acceptor	0.83	0.88
[Al _{Ge}]	acceptor	0.61	1.26
[Ga _{Ge}]	acceptor	0.57	1.26
[In _{Ge}]	acceptor	0.56	1.44

*For Cu, Ga and In as acceptors, the experimental values⁸⁻⁹ are 0.30, 0.31 and 0.40 eV respectively.

**The covalent radii of the host ions : R_{Zn} : 1.31Å, R_{Ge} : 1.22Å.

First Principles Study of Stability, Band Structure and Optical Properties of the ordered $\text{Ge}_{0.50}\text{Sn}_{0.50}$ alloy.

Group IV semiconductor alloys have immense potential for applications in the next generation of Si-based electronic and photonic devices. Alloys and ordered compounds of Si-Ge, Si-Sn and Ge-Sn may have particularly unique optoelectronic properties for applications in quantum-well intersubband technology.¹⁻³ Recently Deng *et al.*⁴ have reported the morphological evolution of an epitaxially strained Ge-Sn alloy thin film on Ge (100) wafers. The surface morphology of the alloy film showed the formation of a pattern of trenches and wires along $\langle 100 \rangle$ direction created by the migration of Sn islands on the growing surface. It is suggested that the high-throughput fabrication of novel nanostructures can be made by forming such trenches on epitaxially strained alloy thin films.

At ambient conditions, both Ge and α -Sn crystallize in the diamond-like phase and are immiscible in the bulk. The equilibrium solid solubility of Sn in Ge is less than 1% while that of Ge in Sn is negligible. In spite of a large lattice mismatch of about 15% between Ge and α -tin, epitaxially-stabilized GeSn thin films have been successfully grown on various substrates. For example, Höchst *et al.*⁵ have prepared crystalline thin films of $\text{Ge}_{1-x}\text{Sn}_x$ on Ge(100) substrates with $x \approx 0.5$. The Sn-rich alloy films, on the other hand, were grown⁶ on InSb and InSb/GaAs substrates having excellent crystallinity for $x < 0.90$ while the Ge-rich alloy films were epitaxially prepared⁷ on Ge (100) for x up to 0.24. On the theoretical front, the nature of the band gap of these alloys have been studied⁸ in the virtual-crystal approximation. The gap is predicted to be direct for $0.3 < x < 0.75$. For $x < 0.3$, the films are expected to exhibit indirect gap while the films with $x > 0.75$ are expected to be metallic, as also observed.⁶

Calculations based on first principles methods are now routinely performed to gain an understanding of structural and electronic properties of a wide variety of materials including

the group IV (e.g. SiGe) binary alloy systems.^{9,10} Since a knowledge of structural, electronic and optical properties of GeSn alloys is critical in promoting the alloy thin films for device applications, we have embarked upon a theoretical study of this alloy system using state-of-the-art linear combination of atomic orbitals (LCAO) method in the framework of density functional theory (DFT). In this paper, we present initial results on the ordered $\text{Ge}_{0.50}\text{Sn}_{0.50}$ alloy in the zincblende phase obtaining its equilibrium structural properties, band structure, dielectric constant and reflectance spectrum.

In the LCAO method a linear combination of Gaussian orbitals are used to construct a localized atomic basis from which Bloch functions are constructed by a further linear combination with plane-wave phase factors. The Gaussian basis sets used here consist of five *s*, four *p* and two *d*-type shells for Ge (i.e. a 97631/ 7631/ 61 set), and seven *s*, six *p* and three *d*-type shells for Sn (i.e. a 9763111/ 763111/ 631 set).¹¹

The total energy calculations are performed in the non-local density approximation to density functional theory (referred to as GGA) with a combination of Becke exchange functional¹² with the Perdew-Wang's correlation functional.¹³ The tolerance on the total energy convergence in the iterative solution of the Kohn-Sham equations is set to 10^{-6} Hartree and a grid of 29 *k*-points was used in the irreducible Brillouin Zone for integration in the reciprocal space. Under these computational conditions, the residual numerical uncertainty in the these calculations is estimated to be about 0.01 eV per atom. The program package CRYSTAL is used for calculations.¹⁴ It has been applied successfully to study bulk and surface properties of covalent materials such as Si, C, BN and GaN.¹⁵⁻¹⁷

We now proceed with the geometry optimization of the GeSn alloy in the zincblende phase assuming that structures and local bonding of the ordered alloy is similar to the constituent elements, namely Ge and α -Sn. The calculated potential energy surface of GeSn together with its elemental components Ge and α -Sn is then fitted to the Vinet equation of state¹⁸ to obtain the equilibrium structural parameters which are listed in Table I. The calculated lattice constant follows the expected trend; the GGA values are about 1.0% larger than the corresponding experimental values for Ge and α -Sn. For the ordered alloy, calculations find

Δa (i.e. $a_{GeSn} - (1/2)(a_{Ge} + a_{Sn})$) to be almost zero obeying Végards linear rule.

The calculated bulk modulus is 53 GPa for $Ge_{0.50}Sn_{0.50}$ while that of Ge and α -Sn is 71 and 42 GPa, respectively (Table I). The experimental values of the bulk modulus for Ge and α -Sn are 77 and 42.6 GPa, respectively.¹⁹ The calculated bulk modulus of the ordered alloy therefore appears to fall on the straight-line average of the constituent elements. The difference (ΔB) between the alloy bulk modulus and the average value B_{avg} (i.e. $(1/2)(B_{Ge} + B_{Sn})$) comes out to be about 1.5 GPa leading the ratio of $\Delta B/B_{avg}$ to be 3%. It is to be noted here that various theoretical calculations reported the $\Delta B/B_{avg}$ ratio to be about 0-2% in SiGe.^{9,20} The bond-strength in the ordered alloy is then predicted to be stiffer than the average of that in the elemental components.

We now calculate the phase stability of the cubic GeSn alloy which is known to depend on the magnitude of the enthalpy of formation (ΔH). Following the notations of Martins and Zunger⁹, ΔH is calculated to be *negative* with a value of 0.068 eV/atom at zero pressure and temperature. In contrast, it is interesting to note here that the LCAO-GGA calculations yield +0.63 and +0.01 eV/atom for ΔH in the cubic alloys of Sn with C and Si, respectively.²¹ The calculated results therefore indicate the relative stability of the GeSn alloy against segregation into the elemental components. Furthermore, calculations of Gibbs free energy show the stability of the cubic phase of GeSn at pressures up to 9 GPa at which one of the alloy components, Ge undergoes a high-pressure phase transition.²²

We now turn our attention to electronic properties of GeSn and display the upper valence and lower conduction band structure of the ordered alloy in Fig. 1. Accordingly, the top of the valence band consists of the triply degenerate Γ_{15} in the absence of the spin-orbit interaction terms in this work. The p states of Ge and Sn forms the upper valence band which has a width of about 6.3 eV. The s states of Ge and Sn form a band with a band-width of 1.6 eV at about 10 eV below the top of the valence band. The Sn $4d$ band appears at about 23 eV below the top of the valence band and is therefore least likely to influence the states in the conduction band (Fig. 2). In the ordered alloy, dispersion of the valence band is similar to that of Ge in agreement with the photoemission study.⁵ However, its conduction

band appears to be similar to that of α -Sn in which the minimum occurs at Γ . The valence band offsets in the alloy components are calculated to be -0.31eV (Ge) and -0.12eV (Sn) with respect to the reference energy of the top of the valence band of the cubic GeSn.

The lowest gap between top of the valence band to bottom of the conduction band is found to be at Γ in the ordered alloy. Thus, the present DFT calculations predict the gap to be direct with a gap value of 0.1 eV. Knowing that the DFT calculations underestimate the band gap relative to experiments, we now estimate the gap from the experimental gap values of the alloy components. α -Sn is a zero-band gap semiconductor while Ge is an indirect-gap semiconductor.^{23,24} The minimum indirect gap in Ge is 0.78 eV associated with the Γ -L transition while the minimum direct gap is 0.98 eV at Γ . Taking the theoretical value of the optical bowing parameter of 0.8eV at Γ , the direct gap (at Γ) in the alloy is estimated²⁰ to be 0.3 eV. It is to be noted here that angle-resolved photoemission study on $\text{Ge}_{0.48}\text{Sn}_{0.52}$ thin films does find a narrowing of the alloy band gap with respect to the average of the gap of its components.⁵

Both valence and conduction level energies at Γ , X and L k-points show a linear variation with applied pressure. The calculated pressure coefficients of these levels listed in Table II yield the coefficient of the minimum-energy direct gap at Γ to be 3.45×10^{-6} eV/bar. At about 7 GPa, a cross-over between the conduction levels at Γ and X occurs resulting into the minimum-energy gap to be indirect in GeSn.

It is well known that the conduction bands are not well described by the density functional theory, though their use in polarizability calculations yield satisfactory values of dielectric response functions in semiconductors.^{16,29} In this work, a sum over states (SOS) method is used to calculate the real and imaginary parts of the polarizability from which related functions such as the dielectric constant and energy loss function (ELF) can easily be obtained. The SOS calculations^{16,28} yield the value of 44.1 \AA^3 for (static) polarizability, 19.6 for dielectric constant and 4.36 for index of refraction of the ordered alloy. At 6889 nm, the index of refraction is calculated to be 4.44 which is very close to the Soref's empirical estimation¹ of 4.52. It is to be noted here that the calculated dielectric constant of 16.0 and

24.3 for Ge and α -Sn are in very good agreement with the reported values²⁶ of 16.0 and 23.8.

The complex dielectric response function is now used to calculate the plasmon energy corresponding to the maximum of the *ELF* function. It is found to be 16.1 eV for GeSn and is smaller than the average of the component values of 19.3 eV and 14.7 eV for Ge and α -Sn, respectively. Our calculated plasmon energy for Ge can be compared with the previously reported value²⁹ of about 17.5 eV where the real part of the dielectric constant was obtained from the imaginary one via the Kramers-Kronig relation. The reflectance, square of the normal incidence reflectivity is determined from the dielectric function via the Fresnel equations, with respect to the incident photon energy for GeSn along with Ge and Sn. As expected, the reflectance behaviour of the ordered alloy can be approximated by the average of the reflectance of Ge and Sn. Similarly, the mean value of the Compton profile²⁷ (with respect to the momentum value q of electron in the scattering direction) of GeSn appears to be the average of that in the elemental components.

In summary, first principles calculations based on the density functional theory find the ordered GeSn alloy to be stable in the zincblende phase up to 9 GPa. The band gap of the cubic alloy is predicted to be direct. Although the bond-strength in the ordered alloy is found to be stiffer than the average of that in the elemental components, the reflectance and Compton profile of the alloy can be obtained by taking the average of their respective values in the elemental components.

REFERENCES

- ¹ R. A. Soref, *J. Vac. Sci. Technol. A* **14**, 913 (1996).
- ² R. A. Soref and L. Friedman, *Superlattices and Microstructures* **14**, 189 (1993).
- ³ R. A. Soref and C. H. Perry, *J. Appl. Phys.* **69**, 539 (1991).
- ⁴ X. Deng, B.-K. Yang, S. A. Hackney, M. Krishnamurthy and D. R. M. Williams, *Phys. Rev. Lett.* **80**, 1022 (1998).
- ⁵ H. Höchst, M. A. Engelhardt and I. Hernández-Calderón, *Phys. Rev. B* **40**, 9703 (1989).
- ⁶ E. A. Fitzgerald, P. E. Freeland, M. T. Asom, W. P. Lowe, R. A. Macharrie, Jr., B. E. Weir, A. R. Kortan, F. A. Thiel, Y.-H Xie, A. M. Sergent, S. L. Cooper, G. A. Thomas and L. C. Kimerling *J. Electronic Materials* **20**, 489 (1991).
- ⁷ O. Gurdal, M.-A. Hasan, M. R. Sardela, Jr., and J. E. Greene, H. H. Radamson, J. E. Sundgren and G. V. Hansson, *Appl. Phys. Lett.* **67**, 956 (1995).
- ⁸ D. W. Jenkins and J. D. Dow *Phys. Rev. B* **36**, 7994 (1987).
- ⁹ J. L. Martins and A. Zunger, *Phys. Rev. Lett.* **56**, 1400 (1986).
- ¹⁰ A. Qteish and R. Resta *Phys. Rev. B* **37**, 1308 (1988).
- ¹¹ We started with basis sets that have been optimized for isolated Ge and Sn atoms by calculating the total energy. In the cubic Ge and Sn lattice, we added a small set of additional Gaussian basis functions to the atomic basis sets. The exponents of the additional functions were optimized by calculating the total energy of a solid. Table I reflects the accuracy of the basis sets for Ge and Sn reproducing the structural properties very well. In the cubic GeSn alloy, the outermost exponents of both Ge and Sn basis sets were further reoptimized. These Basis sets can be obtained from the authors (pandey@mtu.edu).
- ¹² A. D. Becke, *Phys. Rev. A* **38**, 3098 (1988).

- ¹³ J. P. Perdew, and Y. Wang, *Phys. Rev. B* **45**, 13244 (1992).
- ¹⁴ R. Dovesi, V. R. Saunders, C. Roetti, M. Causà, N. M. Harrison, R. Orlando and E. Aprà, *CRYSTAL95 User's Manual*, Universidad de Torino, 1996.
- ¹⁵ R. Pandey, M. Causà, N. M. Harrison and M. Seel, *J. Phys. Condens. Matter* **8**, 3993 (1996).
- ¹⁶ D. Ayma, M. Rérat and A. Lichanot, *J. Phys. Condens. Matter* **10**, 557 (1998).
- ¹⁷ R. Pandey, P. Zapol, P. and M. Causà, *Phys. Rev. B* **55**, 1 (1997)
- ¹⁸ P. Vinet, J. Ferrante, J. H. Rose, and J. R. Smith, *J. Geophys. Res.* **92**, 9319 (1987).
- ¹⁹ R. Ravelo and M. Baskes, *Phys. Rev. Lett.* **79**, 2482 (1997).
- ²⁰ An-Ban Chen and Arden Sher, *Semiconductor Alloys*, Plenum Press, New York, 1995.
- ²¹ R. Pandey, M. Rérat and M. Causà, unpublished.
- ²² M. Baublitz and A. L. Ruoff, *J. Appl. Phys.* **53**, 5669 (1982).
- ²³ S. Groves and W. Paul, *Phys. Rev. Lett.* **11**, 194 (1963).
- ²⁴ M. L. Cohen and J. R. Chelikowsky, *Electronic structure and optical properties of semiconductors*, Springer-Verlag, New York, 1988.
- ²⁵ S. Baroni and R. Resta, *Phys. Rev. B* **33**, 7017 (1986).
- ²⁶ J. C. Phillips, *Phys. Rev. Lett.* **20**, 550 (1968).
- ²⁷ The compton profile was calculated using the impulse approximation. For details, we refer to Ref. 16.
- ²⁸ The SOS method requires calculations of (vertical) transition moments and energies between the valence (occupied) and conduction (unoccupied) states and does not take into account of the relaxation of orbitals due to the perturbative field. Furthermore, the cal-

culated oscillator strengths are required to obey the Thomas-Reiche-Kuhn rule in which transition moments are corrected by a common multiplication factor, thereby making the sum of oscillator strengths to be equal to the number of electrons per unit cell.

²⁹ C. S. Wang and B. M. Klein, *Phys. Rev. B* **24**, 3417 (1981).

TABLES

TABLE I. Structural properties of $\text{Ge}_{0.50}\text{Sn}_{0.50}$, Ge and $\alpha\text{-Sn}$.

		$a(\text{\AA})$	$V(\text{\AA}^3)$	$B(\text{GPa})$	B'
GeSn	This work (GGA)	6.20	59.58	53	6.9
Ge	This work (GGA)	5.74	47.28	71	5.1
	Expt.(Ref. 24)	5.66	45.33	77	--
$\alpha\text{-Sn}$	This work (GGA)	6.65	73.38	42	5.1
	Expt.(Ref. 19)	6.49	68.34	42.6	--

TABLE II. Electronic properties of $\text{Ge}_{0.50}\text{Sn}_{0.50}$ in the zincblende phase.

Band Gap, eV		
Direct	Γ	0.1
	X	3.1
	L	1.6
Indirect	$\Gamma - X$	1.0
	$\Gamma - L$	0.7
Pressure Coefficients, $\times 10^{-6}$ eV/bar		
Valence Band	Γ_{15}	2.40
	X_5	1.13
	L_3	1.85
Conduction Band	Γ_1	5.85
	X_1	1.79
	L_1	3.77